2011

Generation of Broadband Emission by Incorporating N^{3-} into $Ca_3Sc_2Si_3O_{12}:Ce^{3+}$ Garnet for High Rendering White LEDs

Yongfu Liu
Chinese Academy of Sciences

Xia Zhang
Chinese Academy of Sciences

Zhendong Hao
Chinese Academy of Sciences

Xiao-Jun Wang
Georgia Southern University, xwang@georgiasouthern.edu

Jiahua Zhang
Chinese Academy of Sciences

Journal of Materials Chemistry

Cite this: J. Mater. Chem., 2011, 21, 6354

www.rsc.org/materials

PAPER

Generation of broadband emission by incorporating N^{3-} into $Ca_3Sc_2Si_3O_{12}:Ce^{3+}$ garnet for high rendering white LEDs

Yongfu Liu,[ab] Xia Zhang,[a] Zhendong Hao,[a] Xiaojun Wang[c] and Jiahua Zhang*[a]

Received 16th December 2010, Accepted 28th February 2011
DOI: 10.1039/c0jm04404k

Adding Si_3N_4 into green emitting $Ca_3Sc_2Si_3O_{12}:Ce^{3+}$ garnet phosphor generates an additionally red emission band peaking around 610 nm that are assigned to Ce^{3+} ions having N^{3-} in their local coordination. The excitation spectrum of the red band consists of not only a distinct band at 510 nm of itself but also an intense blue band at 450 nm that belongs to the typical Ce^{3+} ions with green emission, indicating a notable energy transfer from the green emitting Ce^{3+} ions to the red ones. The energy transfer significantly enables the achievement of a broad emission spectrum covering a red and green spectral region suitable for generating white light upon a blue light-emitting diode (LED) excitation. The decay patterns of the red and green fluorescence are discussed in relation to the effect of energy transfer. A white LED with high color rendering of 86 and low correlated color temperature of 4700 K is fabricated using the present single garnet phosphor.

1. Introduction

Phosphor converted white light emitting diodes (pcWLEDs) are potential replacements for conventional light sources such as incandescent or fluorescent lamps.[1–4] The most current pcWLEDs employ yellow emitting $Y_3Al_5O_{12}:Ce^{3+}$ ($YAG:Ce^{3+}$) garnet phosphor combined with blue InGaN LEDs.[5–7] Due to deficient emission in the red spectral region, $YAG:Ce^{3+}$ phosphor limits the color rendering index (CRI) of pcWLEDs below 80, in comparison to CRIs of 100 for incandescent lamps and 82–85 for fluorescent lamps.[8–10] To achieve higher CRIs (>80), many studies have been devoted to development of efficient red phosphors, such as $(Sr,Ba)_2Si_5N_8:Eu^{2+}$,[11] $CaAlSiN_3:Eu^{2+}$,[12] $Lu_2CaMg_2Si_3O_{12}:Ce^{3+}$,[13] and our previously developed $Ca_2P_2O_7:Eu^{2+},Mn^{2+}$.[14] However, these phosphors have to be blended with other yellow or green emitting phosphors to fabricate pcWLEDs, which suffer from energy loss due to reabsorption between different phosphors.

A single white phosphor instead of phosphor blends could be beneficial to improve optical properties of pcWLEDs. For this purpose, significant investigations have been done to modify $YAG:Ce^{3+}$ phosphor by introducing red emitting centers that are able to effectively accept energies transferred from yellow emitting Ce^{3+} centers. Mueller-Mach *et al.*[15] added Pr^{3+} into $YAG:Ce^{3+}$ by substitution for Y^{3+} sites and consequently obtained a red emission line at 608 nm, originating from $^1D_2 \rightarrow {}^3H_4$ transition of Pr^{3+} through Ce^{3+}–Pr^{3+} energy transfer. Due to concentration quenching, the area intensity of the red line is not enough to balance the spectra for notably improving CRI. Recently, Setlur *et al.*[16] demonstrated an example that red emitting Ce^{3+} sites are created by incorporating Si^{4+}-N^{3-} into $(Lu,Y,Tb)_3Al_5O_{12}:Ce^{3+}$ aluminate garnet phosphors. The new sites are assigned to Ce^{3+} ions with N^{3-} in their coordination where O^{2-} with a larger electronegativity is replaced by N^{3-} with a lower electronegavity leading to an enhanced polarizability and red shift of the lowest 5d level of Ce^{3+}. The CRIs over 80 were expected for the pcWLEDs using the modified single aluminate garnet phosphor which is composed of both yellow and red emitting Ce^{3+} sites. Besides $YAG:Ce^{3+}$, we notice that a new green emitting silicate garnet phosphor $Ca_3Sc_2Si_3O_{12}:Ce^{3+}$ ($CSS:Ce^{3+}$)[17] has been developed recently that exhibits highly efficient luminescence and high thermal stability superior to $YAG:Ce^{3+}$, however, suffering from deficient red emission for pcWLEDs. Obviously, to modify the emission spectrum of this green phosphor by enriching its red emission component is a significant alternative for achieving a single white phosphor.

In this paper, we report the generation of red emitting Ce^{3+} sites in green emitting $CSS:Ce^{3+}$ by adding N^{3-} to replace O^{2-}. Possible charge compensation mechanisms of N^{3-} and O^{2-} are discussed. A notable energy transfer from the typical green emitting Ce^{3+} sites to the red emitting Ce^{3+} sites takes place, resulting in a broadband emission. A high CRI of 86 is achieved in the pcWLEDs using the single garnet phosphor.

[a]*Key Laboratory of Excited State Processes, Changchun Institute of Optics, Fine Mechanics and Physics, Chinese Academy of Sciences, 3888 Eastern South Lake Road, Changchun, 130033, China. E-mail: zhangjh@ciomp.ac.cn; Fax: +86-0431-86708875; Tel: +86-0431-86708875*
[b]*Graduate School of Chinese Academy of Sciences, Beijing, 100039, China*
[c]*Department of Physics, Georgia Southern University, Statesboro, Georgia, 30460, USA*

2. Experimental

2.1 Materials and synthesis

Samples with nominal compositions of $Ca_{2.97}Sc_2Si_3O_{12-6x}N_{4x}:0.03Ce^{3+}$ (x = 0–0.8) were prepared using mixtures of high purity $CaCO_3$, Sc_2O_3, SiO_2, CeO_2, and α-Si_3N_4 and sintered in a tubular furnace at 1100–1300 °C for 4–6 h in reductive atmosphere (10% H_2 + 90% N_2 mixed flowing gas).

2.2 Materials characterization

Powder X-ray diffraction (XRD) data were collected using Cu-Kα radiation (λ = 1.54056 Å) on a Bruker D8 Advance diffractometer. The photoluminescence (PL), photoluminescence excitation (PLE) and diffuse reflectance (DR) spectra were measured using a HITACHI F-4500 spectrometer. The fluorescence decay curves were measured by FL920 Fluorescence Lifetime Spectrometer with the time resolution of 2 ns. The chromaticity coordinates, color rendering index (CRI) and the correlated color temperature (CCT) of white LEDs were measured using Ocean Optics USB4000 Spectrometer.

3. Results and discussion

Fig. 1 shows the XRD patterns for phosphors with nominal compositions of $Ca_{2.97}Sc_2Si_3O_{12-6x}N_{4x}:0.03Ce^{3+}$ (x = 0–0.8). The primary phases in all of these samples are CSS garnets (JCPDF No. 72-1969 CSS) but with a small amount of Sc_2O_3 phase (JCPDF No. 74-1210 Sc_2O_3). Suzuki *et al.* also pointed out that it is difficult to obtain a pure CSS phase by the solid-state reaction method.[18] With regard to Ce^{3+}, extended X-ray absorption fine structure (EXAFS) analysis showed the occupied site of Ce^{3+} to be the Ca^{2+} site in the CSS for the ionic radius of Ce^{3+} is close to that of Ca^{2+}.[17] To understand the mechanism for the replacement of a smaller O^{2-} by a larger N^{3-}, the garnet lattice parameters are calculated using the XRD data (Table 1). It is found the lattice does not increase monotonously with increasing x, but shrinks for $x \leq 0.5$. As a result, charge compensation mechanism may play an important role in the variation of lattice parameters. To compensate the charge differences of N^{3-} and O^{2-}, possible compensation mechanisms may take place, which include oxidation of Ce^{3+} to Ce^{4+}, substitution of Ca^{2+} by Ce^{3+} or Sc^{3+}, Sc^{3+} by Si^{4+} and formation of oxygen vacancies. The effect of Ce^{4+} and the substitution of Ca^{2+} by Ce^{3+} could be neglected for the doping concentration of Ce (0.03) is much lower than the nominal content of N (0.4–3.2) and the absorption of Ce^{3+} does not reduce with increasing x as the DR spectra shows in Fig. 3. We notice that the XRD peak for Sc_2O_3 grows up with increasing x, implying that the substitution of Sc^{3+} by Si^{4+} might be a compensation mechanism rather than that of Ca^{2+} by Sc^{3+}. The difference between the ionic radius of Sc^{3+} (0.745 Å) and Si^{4+} (0.42 Å) is 0.325 Å smaller than that (0.39 Å) between N^{3-} (1.71 Å) and O^{2-} (1.32 Å). This means substitution of Sc^{3+} by Si^{4+} can not completely compensate the lattice increment due to replacement of O^{2-} by N^{3-}. Thus, the formation of oxygen vacancies is considered to be another charge compensation mechanism, which can result in the reduction of lattice parameters.[19] Discussions on oxygen vacancies will be performed latter in combination with the results shown in Fig. 3 and Fig. 8. Based on the behavior of the XRD and the lattice parameters on x, we infer that the substitution of Sc^{3+} by Si^{4+} and the formation of oxygen vacancies take place to compensate for the replacement of O^{2-} by N^{3-}. For $x \leq 0.5$, the formation of oxygen vacancies leads to the reduction of lattice parameters. For $x \geq 0.5$, the formation of oxygen vacancies reaches saturation, exhibiting increase of the lattice parameters with x.

Fig. 2 shows the normalized PL spectra upon 450 nm excitation for the N^{3-} contained CSS : Ce^{3+} phosphors with nominal

Table 1 Lattice parameter (Å) of $Ca_{2.97}Sc_2Si_3O_{12-6x}N_{4x}:0.03Ce^{3+}$($x$ = 0–0.8)

Sample	$Ca_{2.97}Sc_2Si_3O_{12-6x}N_{4x}:0.03Ce^{3+}$					
x	0	0.1	0.3	0.5	0.6	0.8
Lattice parameter (Å)	12.2257	12.2138	12.2175	12.2244	12.2316	12.2590

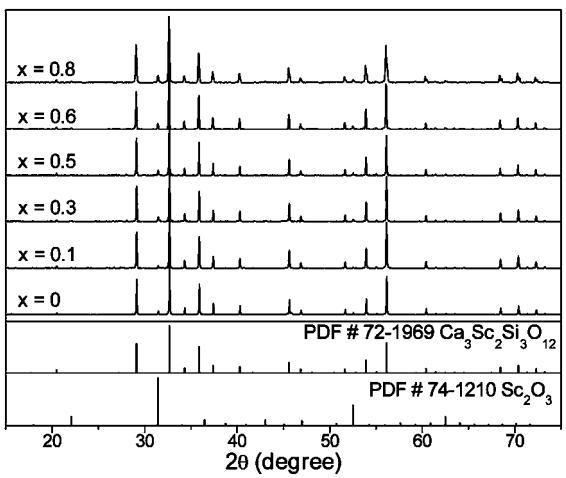

Fig. 1 XRD patterns for phosphors with nominal compositions of $Ca_{2.97}Sc_2Si_3O_{12-6x}N_{4x}:0.03Ce^{3+}$ (x = 0–0.8).

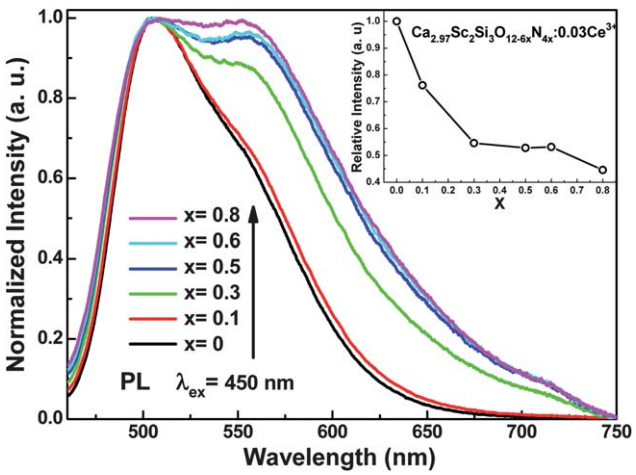

Fig. 2 PL spectra and relative intensity (inset) under 450 nm excitation for phosphors with nominal compositions of $Ca_{2.97}Sc_2Si_3O_{12-6x}N_{4x}:0.03Ce^{3+}$ (x = 0–0.8).

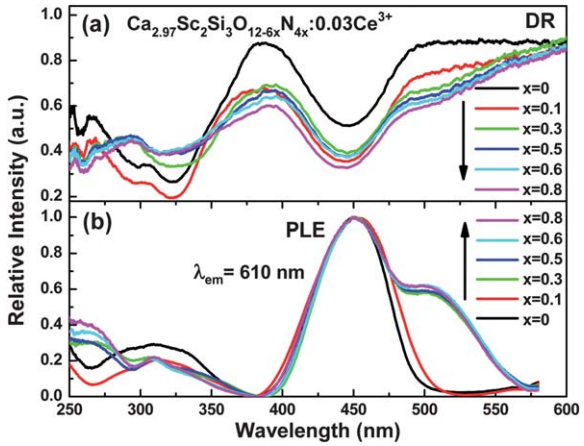

Fig. 3 DR (a) and PLE (b) spectra for phosphors with nominal compositions of $Ca_{2.97}Sc_2Si_3O_{12-6x}N_{4x}$: 0.03Ce^{3+} (x = 0–0.8).

compositions of $Ca_{2.97}Sc_2Si_3O_{12-6x}N_{4x}$: 0.03Ce^{3+} (x = 0–0.8). The N^{3-} free CSS : Ce^{3+} shows a typical green emission band peaking around 500 nm. Addition of N^{3-} to CSS : Ce^{3+} results in a great enhancement in the longer wavelength side of the typical green band in the emission spectra, correspondingly leading to luminescent color changing from green to yellow-orange. Meanwhile, as Fig. 1 shows, the relative integral emission intensities decrease with increasing x. The integral emission intensities for N free CSS : Ce can reach as high as 106% compared with YAG : Ce at the same excitation wavelength 450 nm. As discussed above, the substitution of Si^{4+} by Sc^{3+} and the generation of oxygen vacancies are possible charge compensation mechanisms between N^{3-} and O^{2-}, resulting in the formation of defects in the CSS host. More defects are formed in the CSS host with increasing x, therefore, more reductions of the phosphor emission intensities take place.

Fig. 3 shows the DR (a) and PLE (b) spectra of the phosphors. The N^{3-} free sample appears at a typical absorption band and a corresponding PLE band around 450 nm, which is generally due to 4f → 5d transition of Ce^{3+} in the CSS. One can find the N^{3-} contained samples exhibit an additional distinct absorption band and a corresponding PLE band around 510 nm, which is about 2600 cm^{-1} lower in energy *versus* the original PLE band at 450 nm. The relative strength of the low energy absorption band is correlated to the amount of N^{3-} addition. According to the results of the Si^{4+}-N^{3-} incorporated $(Lu,Y,Tb)_3Al_5O_{12}$: Ce^{3+} reported by Setlur *et al.*,[16] the present low energy absorption band is attributed to the 4f → 5d transition of Ce^{3+} ions which have N^{3-} in their nearest neighbor coordination.

Fig. 4 shows the PL and PLE spectra for $Ca_{2.97}Sc_2Si_3O_{7.2}N_{3.2}$: 0.03Ce^{3+}. One can observe the emission spectra shift strongly toward the red side with tuning the excitation wavelength from the position of high energy PLE band to low energy PLE band. When only the low energy PLE band is excited either by 510 nm or 550 nm, there appears an identical red emission band peaking around 610 nm, which no longer changes with further increasing excitation wavelengths from 510 nm (Fig. 4c). Considering that a few of Sc_2O_3 phase exists in the present phosphors, we notice that the emission spectrum of Sc_2O_3 : Ce^{3+} is a band around 580 nm reported by Feofilov *et al.*[20] It is different from the observed red emission band at

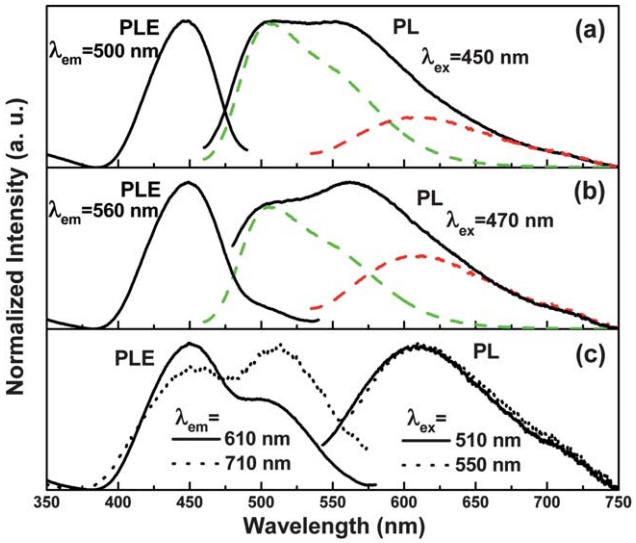

Fig. 4 PL and PLE spectra under various excitation and monitoring wavelengths for phosphor $Ca_{2.97}Sc_2Si_3O_{7.2}N_{3.2}$: 0.03Ce^{3+}.

610 nm. As a result, the distinct red emission band is just due to the Ce^{3+} ions with N^{3-} in their coordination. It is found that the emission spectra for various excitation wavelengths can be decomposed into a typical green emission of Ce^{3+} in CSS and a red emission of Ce^{3+} with N^{3-} in its coordination, as shown in Fig. 4a and 4b. In addition, the excitation spectrum of the red emission band monitoring at 710 nm, where CSS : Ce^{3+} has no emission, not only consists of the low energy PLE band at 510 nm but also an intense high energy PLE band at 450 nm of the typical Ce^{3+}. This directly indicates an effective energy transfer from the high energy Ce^{3+} to the low energy one. The necessary condition for the energy transfer is presented clearly in Fig. 4 that the typical green emission band overlaps well with the PLE band of the red emission.

The effect of energy transfer is also presented in the fluorescence decay curves as shown in Fig. 5. The decay curve of the green fluorescence at 500 nm is exponential in N^{3-} free CSS : Ce^{3+} with

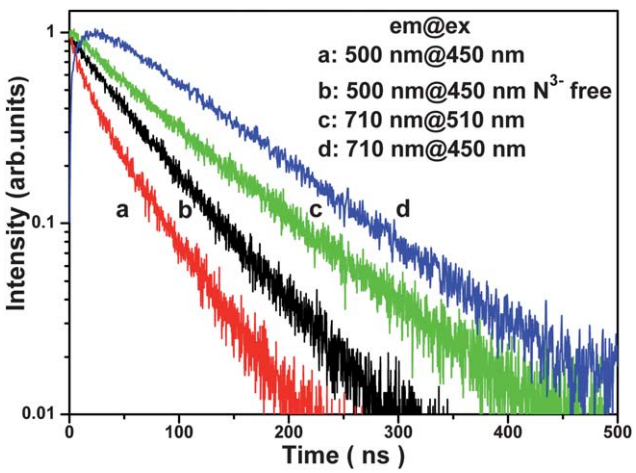

Fig. 5 Fluorescence decay profiles with various excitation wavelengths and various monitoring wavelengths for $Ca_{2.97}Sc_2Si_3O_{7.2}N_{3.2}$: 0.03Ce^{3+} (a, c, d) and N^{3-} free CSS : Ce^{3+} (b) phosphors.

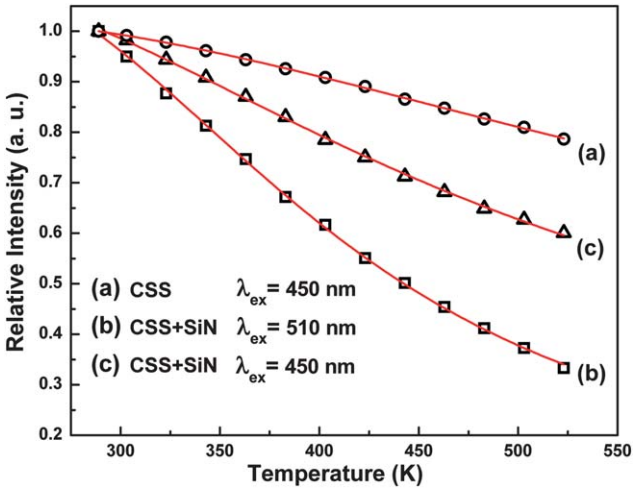

Fig. 6 Relative emission intensity *versus* temperature for the typical green phosphor (CSS) and $Ca_{2.97}Sc_2Si_3O_{7.2}N_{3.2}$: $0.03Ce^{3+}$ (CSS + SiN) under various excitation wavelengths.

a lifetime τ_0 of 57 ns (b), but non-exponential in N^{3-} contained CSS : Ce^{3+} that can be well fit by using a bi-exponential function with a short lifetime of 12 ns and a tail lifetime of 50 ns (a). The non-exponential decay yields an average lifetime τ to be 35 ns, which is calculated by integrating the area under the decay curve with a normalized initial intensity. Meanwhile, the decay curve of the red fluorescence at 710 nm in N^{3-} contained CSS : Ce^{3+} shows an exponential function with a lifetime of 95 ns upon pulsed excitation at 510 nm (c), but a rising edge followed by a decay with a tail lifetime of 95 ns upon pulsed excitation at 450 nm (d). The rising time is close to the short lifetime of the green fluorescence. The results presented in Fig. 9 further confirm the energy transfer from the green emitting Ce^{3+} to the red emitting Ce^{3+}. The transfer efficiency for 450 nm excitation is evaluated to be 38% from $1 - \tau/\tau_0$. One notices that the rising edge of the red fluorescence dose not start from zero, suggesting that a part of red

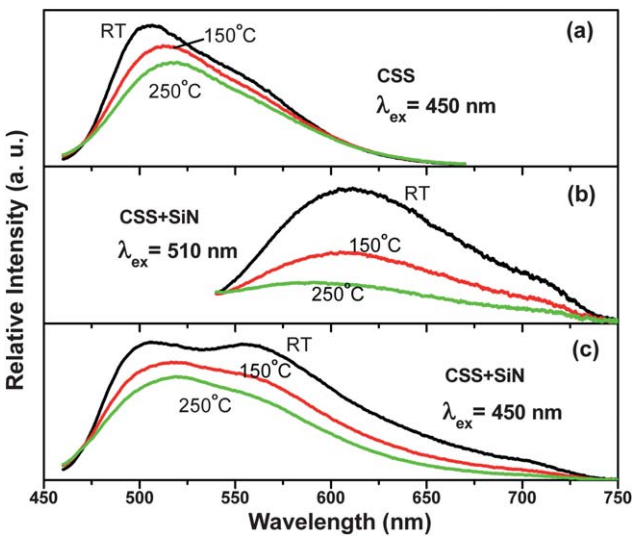

Fig. 7 PL spectra *versus* temperature for the typical green phosphor (CSS) and $Ca_{2.97}Sc_2Si_3O_{7.2}N_{3.2}$: $0.03Ce^{3+}$ (CSS + SiN) under various excitation wavelengths.

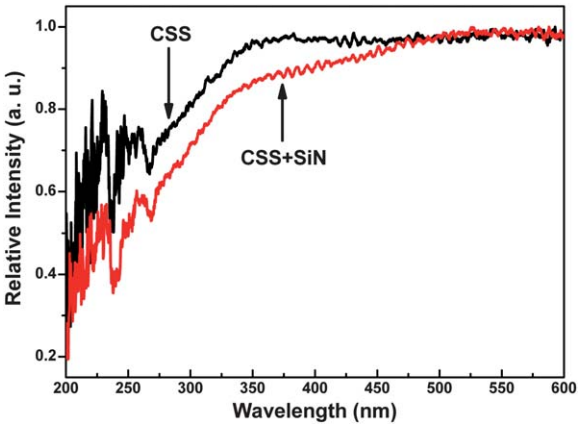

Fig. 8 DR spectra for host materials CSS and $Ca_3Sc_2Si_3O_{7.2}N_{3.2}$ (CSS + SiN).

emitting Ce^{3+} can be directly excited by 450 nm due to the broad PLE band at 510 nm. The energy transfer significantly enables the achievement of a broad emission spectrum, especially for 470 nm excitation (Fig. 4b), covering a red and green spectral region suitable for generating white light upon a blue LED excitation.

Fig. 6 shows the thermal quenching of the integral emission intensities for the CSS and the N^{3-} incorporated CSS phosphors, in which the integral emission intensities at room temperature (RT) are set as normalized. It is obvious that the CSS phosphor shows good thermal quenching characteristics under blue light (450 nm) excitation (a). However, under green light (510 nm) excitation, intensities of the red Ce^{3+} emissions for the N^{3-} incorporated phosphor reduce largely at high temperature (b), resulting in a fast attenuation of overall luminescence in the N^{3-} incorporated phosphor (c) compared to the CSS phosphor (a). The fast attenuation does not reflect the characteristics of the green component because the green components for both phosphors reduce slowly against heat as shown in Fig. 7. Moreover, with increasing temperature, the green emissions for both phosphors (Fig. 7a and 7c) exhibit a redshift and the red emissions for N^{3-} incorporated phosphor (Fig. 7b) exhibit a blueshift.

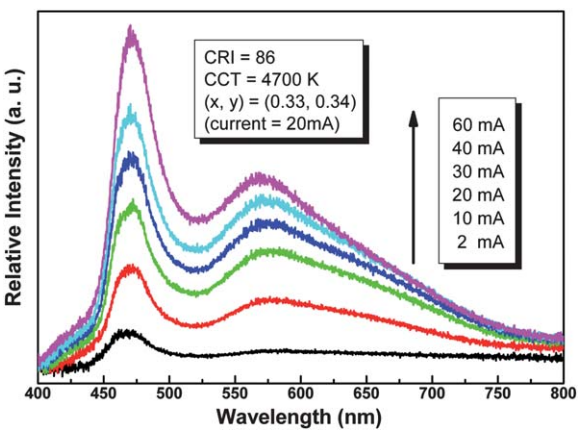

Fig. 9 Emission spectra of a white LED fabricated using a blue InGaN LED chip (λ_{ex} = 470 nm) and $Ca_{2.97}Sc_2Si_3O_{7.2}N_{3.2}$: $0.03Ce^{3+}$ phosphor under different forward bias currents (indicated).

The strong quenching behavior of the red band may be understood by analyzing the DR spectra of the phosphors (Fig. 8). $Ca_3Sc_2Si_3O_{7.2}N_{3.2}$ has an absorption band edge from 450 nm (~2.76 eV), whereas CSS is from 350 nm (~3.54 eV). The lower absorption band edge may provide an effective quenching pathway for the 5d excited state of Ce^{3+} in N^{3-} incorporated phosphor. The low energy absorption can be originated from the oxygen vacancies that are generated as compensation for the replacement of O^{2-} by N^{3-} as discussed previously. This low energy absorption around 450 nm can be also observable as a background in the DR spectra in Fig. 3. The background enhances remarkably for small x, correlating to the former discussion on the formation of oxygen vacancies.

Fig. 9 shows the emission spectra of a pcWLED fabricated with the $Ca_{2.97}Sc_2Si_3O_{7.2}N_{3.2} : 0.03Ce^{3+}$ single phosphor coated on an InGaN LED ($\lambda_{ex} = 470$ nm) chip under different forward bias currents. The white LED shows the Commission International de I'Eclairage (CIE) chromaticity coordinates in the range of $x = 0.32$–0.35 and $y = 0.32$–0.36, CCTs in the range of 4700–5600 K and CRIs in the range of 82–86. When the forward current is 20 mA, the white LED shows high CRI of 86 and low CCT of 4700 K with luminous efficiency of 50 lm/W. The N^{3-} incorporated CSS : Ce^{3+} exhibits unique spectroscopic properties superior to YAG : Ce^{3+} for high CRIs and low CCTs of pcWLEDs.

4. Conclusions

In summary, the addition of N^{3-} into CSS : Ce^{3+} leads to a distinct low energy absorption band around 510 nm and a red emission band peaking at 610 nm compared to the typical Ce^{3+} absorption band at 450 nm and the green emission band at 500 nm. The red band is attributed to the Ce^{3+} ions with N^{3-} in their coordination in the CSS. The substitution of Sc^{3+} by Si^{4+} and the formation of oxygen vacancies take place to compensate for the replacement of O^{2-} by N^{3-}. The emission spectrum in the N^{3-} incorporated CSS : Ce^{3+} can be decomposed into the typical green emission band and the new red emission band. A notable energy transfer from the green emitting Ce^{3+} with a lifetime of $\tau \sim 50$ ns to the red emitting one with a lifetime of $\tau \sim 95$ ns is demonstrated. The performance of energy transfer enables a broad band emission upon blue light excitation to be obtained. A white LED with high CRI of 86 is fabricated using the present N^{3-} contained single CSS garnet phosphors. The strong thermal quenching of the red emission Ce^{3+} ions could affect the efficiency and color of pcWLEDs. The present phosphor still could be a promising candidate as a single white phosphor for pcWLEDs with high CRI and low CCT.

Acknowledgements

This work is financially supported by the National Nature Science Foundation of China (10834006, 10774141, 10904141, 10904140), the MOST of China (2006CB601104), the Scientific project of Jilin province (20090134, 20090524) and CAS Innovation Program.

References

1 S. Nakamura, T. Mukai and M. Senoh, *Appl. Phys. Lett.*, 1994, **64** (13), 1687–1689.
2 E. F. Schubert and J. K. Kim, *Science*, 2005, **308**, 1274–1278.
3 Y. C. Chiu, W. R. Liu, C. K. Chang, C. C. Liao, Y. T. Yeh, S. M. Jang and T. M. Chen, *J. Mater. Chem.*, 2010, **20**, 1755–1758.
4 N. Guo, H. P. You, Y. H. Song, M. Yang, K. Liu, Y. H. Zheng, Y. J. Huang and H. J. Zhang, *J. Mater. Chem.*, 2010, **20**, 9061–9067.
5 D. Haranath, H. Chander, P. Sharma and S. Singh, *Appl. Phys. Lett.*, 2006, **89**, 173118.
6 K. Sakuma, K. Omichi, N. Kimura, M. Ohashi, D. Tanaka, N. Hirosaki, Y. Yamamoto, R.-J. Xie and T. Suehiro, *Opt. Lett.*, 2004, **29**(17), 2001–2003.
7 W. B. Im, N. N. Fellows, S. P. DenBaars and R. Seshadri, *J. Mater. Chem.*, 2009, **19**, 1325–1330.
8 H. S. Jang, W. B. Im, D. C. Lee, D. Y. Jeon and S. S. Kim, *J. Lumin.*, 2007, **126**, 371–377.
9 Y. Chen, M. Gong, G. Wang and Q. Su, *Appl. Phys. Lett.*, 2007, **91**, 071117.
10 R. J. Xie, N. Hirosaki, K. Sakuma, Y. Yamamoto and M. Mitomo, *Appl. Phys. Lett.*, 2004, **84**, 5404–5406.
11 M. Zeuner, P. J. Schmidt and W. Schnick, *Chem. Mater.*, 2009, **21**, 2467.
12 K. Uheda, N. Hirosaki, Y. Yamamoto, A. Naito, T. Nakajima and H. Yamamoto, *Electrochem. Solid-State Lett.*, 2006, **9**, H22.
13 A. A. Setlur, W. J. Heward, Y. Gao, A. M. Srivastava, R. G. Chandran and M. V. Shankar, *Chem. Mater.*, 2006, **18**, 3314–3322.
14 Z. D. Hao, J. H. Zhang, X. Zhang, X. Y. Sun, Y. S. Luo and S. Z. Lu, *Appl. Phys. Lett.*, 2007, **90**, 261113.
15 R. Mueller-Mach, G. O. Mueller, M. R. Krames and T. Trottier, *IEEE J. Sel. Top. Quantum Electron.*, 2002, **8**, 339–345.
16 A. A. Setlur, W. J. Heward, M. E. Hannah and U. Happek, *Chem. Mater.*, 2008, **20**, 6277–6283.
17 Y. Shimomura, T. Honma, M. Shigeiwa, T. Akai, K. Okamoto and N. Kijima, *J. Electrochem. Soc.*, 2007, **154**(1), J35–J38.
18 Y. Suzuki, M. Kakihana, Y. Shimaomura and N. Kijima, *J. Mater. Sci.*, 2008, **43**, 2213–2216.
19 Y. H. Liu, W. D. Zhuang, Y. S. Hu and W. G. Gao, *J. Rare Earths*, 2010, **28**(2), 181–184.
20 S. P. Feofilov, D. V. Arsentyev, A. B. Kulinkin and R. I. Zakharchenya, *J. Lumin.*, 2011, **131**(3), 438–441.

